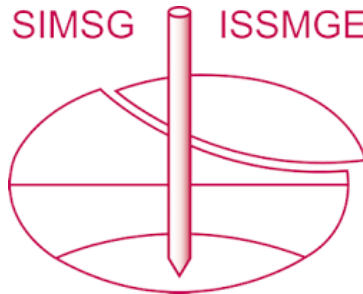


INTERNATIONAL SOCIETY FOR SOIL MECHANICS AND GEOTECHNICAL ENGINEERING



This paper was downloaded from the Online Library of the International Society for Soil Mechanics and Geotechnical Engineering (ISSMGE). The library is available here:

<https://www.issmge.org/publications/online-library>

This is an open-access database that archives thousands of papers published under the Auspices of the ISSMGE and maintained by the Innovation and Development Committee of ISSMGE.

The paper was published in the proceedings of the 10th European Conference on Numerical Methods in Geotechnical Engineering and was edited by Lidija Zdravkovic, Stavroula Kontoe, Aikaterini Tsiampousi and David Taborda. The conference was held from June 26th to June 28th 2023 at the Imperial College London, United Kingdom.

To see the complete list of papers in the proceedings visit the link below:

<https://issmge.org/files/NUMGE2023-Preface.pdf>

Accuracy and efficiency of explicit substepping scheme for complex soil models in finite element framework

Y.P. Dong

Department of Environmental and Resource Engineering, Technical University of Denmark, Kgs. Lyngby, Denmark

ABSTRACT: This paper describes the algorithm used to integrate a complex elastoplastic constitutive model for clays, the MIT-E3, in the finite element framework, followed by extensive evaluations. The explicit substepping scheme with different order of accuracy is adopted in the integration due to its simplicity, and also because of complexities in the model formulation. The numerical integration is validated by reproducing the stress-strain behaviour in single element tests, and also by checking the error behaviour with the order of accuracy of the integration method. The accuracy and efficiency of different methods in the integration are evaluated in a rigorous and consistent manner, which has practical implication for choosing suitable methods and parameters in the analysis. The substepping scheme with error control is shown to be stable in the challenging geotechnical problems, while the efficiency is affected by the strain increment size which is problem dependent.

Keywords: Constitutive models, integration, finite element method

1 INTRODUCTION

Advanced constitutive models for soils are essential to achieve reliable results in numerical analysis of geotechnical problems (e.g. excavations, slopes, and foundations), but their implementation in nonlinear finite element programs should be accurate, efficient, and robust. In the last decades, significant efforts have been made to develop constitutive models which can describe complex aspects of saturated clay behavior observed in laboratory tests including (i) anisotropic stress-strain-strength path, (ii) nonlinear and inelastic properties of overconsolidated soils, (iii) response under cyclic loading, (iv) time and rate dependent behavior, and (v) structural and fabric effects. A plethora of soil models have been developed in the literature to represent the sophisticated clay behavior with various levels of capabilities and complexity. The MIT-E3 (Whittle and Kavvasdas 1994) is one of those complex elastoplastic models, and its performance has been evaluated for predicting the rate-independent behavior of K_0 normally to moderately overconsolidated clays (Whittle 1993, Whittle et al. 1994). The overall high quality of the predictions has provided the basis for implementing the model in a general nonlinear finite element program for broad geotechnical applications.

This paper describes the explicit substepping scheme used to integrate the MIT-E3 model in a general finite element program, AbaqusTM, and evaluates its performance (i.e. accuracy, efficiency, and stability) in nonlinear analyses. The explicit substepping scheme has been used for relatively simple constitutive models (e.g., the Mohr-Coloumb model (Sloan 1987), and the

critical state family (Sloan et al. 2001, Lloret-Cabot et al. 2016, 2021)), but can be very challenging for complex models (e.g. MIT-E3) due to various model specific features. The original implementation (Hashash 1992) has limitations (e.g. efficiency and stability), and numerical issues have been encountered in complex nonlinear analyses. Therefore, a completely new implementation was conducted recently using more rigorous and efficient explicit substepping scheme with error controls.

The integration is validated through reproducing the stress-strain behaviour from typical element tests for soils (e.g. triaxial compression and extension). The accuracy and efficiency of the integration scheme are evaluated against the order of accuracy for each integration method and the number of substeps used for a strain increment. This procedure can further verify the correctness of the integration, and provides guidance in selecting suitable tolerances to balance accuracy and efficiency for practical applications. The general performance (e.g. accuracy, efficiency, and stability,) is demonstrated through the deeply-embedded rigid pile/pipe section analysis in both isotropic bedding plane and anisotropic depositional plane.

2 FORMULATION OF THE MIT-E3 MODEL

2.1 Model formulation and key features

MIT-E3 model was developed to describe the rate-independent behavior of overconsolidated clays under cyclic loading, based on the observation of

experimental data of soils. The formulation of the MIT-E3 model was described in Whittle and Kavvas (1994), and in Whittle (1995) with corrections of some equations.

In general, the model formulation comprises three components: (1) an elastoplastic model for normally consolidated clay including anisotropic and strain-softening behaviour (Kavvas 1982); (2) nonlinear paraelastic equations (Hueckel and Nova 1979) to describe the small strain nonlinearity and hysteretic response in unloading and reloading; and (3) bounding surface plasticity (Krieg 1975, Dafalias and Popov 1975) for irrecoverable, anisotropic and path dependent behaviour of overconsolidated clays. Extensive comparisons with measured data from undrained shear tests performed in different modes (e.g. triaxial, plane strain, and simple shear) of shearing show that the model gives excellent predictions of conditions at maximum shear stress and describes accurately the nonlinear shear stress-strain behaviour (Whittle 1993).

2.2 Constitutive equations

The rate-form (incrementally linearized) constitutive equations are presented in Whittle and Kavvas (1994), including the physical meaning and suggested procedures for determining the 15 input constants. Additional state variables are required to describe the state of the model (e.g. location of the yield surface and bounding surfaces, and the stress reversal point).

3 INTEGRATION FRAMEWORK

Three methods in the explicit substepping integration scheme are adopted in the implementation to evaluate their performance in complex soil models, (1) the forward Euler (FE) substepping method, (2) the modified Euler (ME) substepping method with error control, and (3) the Runge-Kutta (RK) substepping method with error control. Particular interests include the accuracy, efficiency and stability of these methods in nonlinear analyses. Moreover, a procedure is needed to select appropriate tolerances to balance the accuracy and efficiency in practical applications.

The FE substepping method divides the strain increment into equal-sized subincrement, and integrates the constitutive equations using multiple steps. The procedure for the single step FE update is described in Figure 1. Several key issues have to be addressed carefully in the integration process, (i) stress reversal point check, (ii) monotonic loading or reversed unloading determination, (iii) state update within the bounding surface using mapping rules, (iv) intersection with bounding surface from overconsolidated state using the Pegasus algorithm (Dowell and Jarratt 1972), and (v) state update on the bounding surface and consistent drift correction.

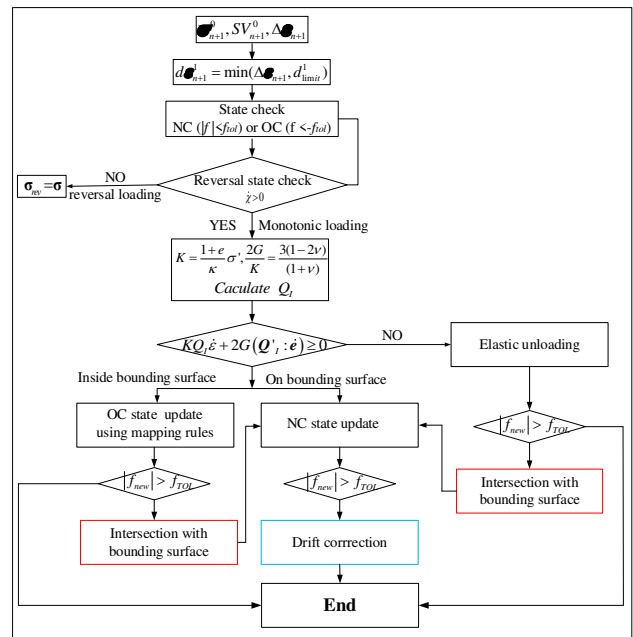


Figure 1. Flowchart of single step FE integration method

The ME and RK methods use multiple stages of FE evaluations, but the substepping size is adjusted automatically based on the error estimate and specified tolerance. The final state variables are the weighted average of the FE updates, with equations summarised in Dormand and Prince (1980). More details of the error estimate and step size determination are described in Sloan et al. (2001).

4 VERIFICATION OF THE INTEGRATION ON SINGLE ELEMENT TESTS

4.1 Triaxial shear tests

A relatively small substepping size, $d_{limir} = 10^{-6}$, is adopted for the FE method, while a moderate error tolerance for the substepping size, $S_{TOL} = 10^{-6}$, is chosen for the ME and RK methods with error control, considering the balance between accuracy and efficiency. A tight yield function tolerance, $f_{TOL} = 10^{-10}$, is used for all integration methods to enforce the consistency condition.

Figure 2 shows the computed effective stress paths and stress-strain response for the K_0 -consolidated undrained triaxial compression (CK₀UC) and extension (CK₀UE) tests for Boston Blue Clay (BBC) with four initial overconsolidation ratios (OCR = 1, 2, 4, and 8). In these tests, the sample is consolidated in K_0 condition and rebounded to the respective OCR levels, and then sheared up to a total axial strain 10%, following the SHANSEP procedure (Ladd and Foott 1974). It shows again that all three integration methods can produce accurate results in triaxial conditions that are comparable and consistent with the reported data in Whittle (1993).

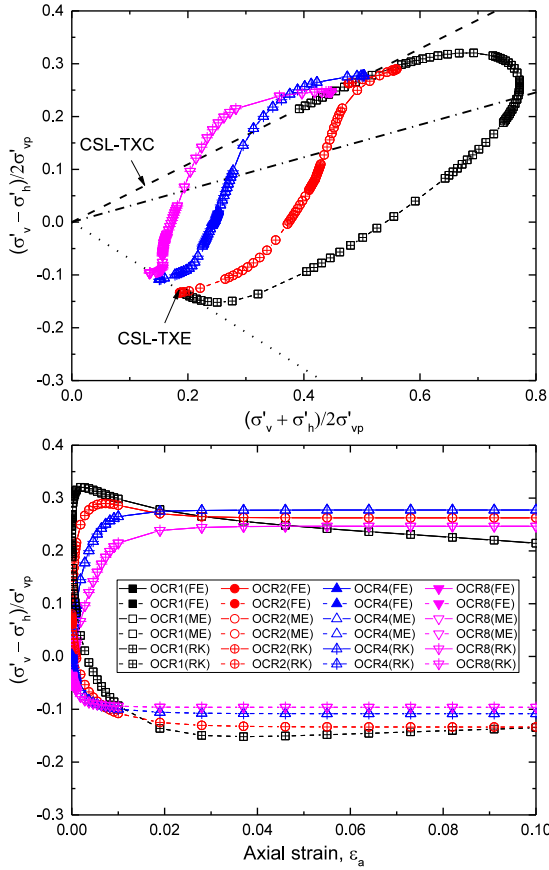


Figure 2. Computed K_0 -consolidated triaxial compression and extension tests

5 ACCURACY AND EFFICIENCY OF THE INTEGRATION

5.1 Error indicator

For a single load step or iteration in finite element analysis, inexact integration of the constitutive equations will lead to errors in the computed stresses, and these errors will propagate throughout the finite element grids after a number of load steps or iterations. In the current work these errors are measured directly by monitoring the computed stress σ , using the relative error, err , defined in Equation (1),

$$err = \frac{|\sigma - \sigma_{ref}|}{|\sigma_{ref}|} \quad (1)$$

where σ_{ref} is the reference stress either from exact solution or computed using a highly accurate scheme for integrating the constitutive equations.

5.2 Accuracy and efficiency in element tests

As suggested in Lloret-Cabot *et al.* (2016), the cleanest comparison between different integration schemes is to consider the solution for stresses approximated by each numerical method in a single elastoplastic loading increment starting at a known initial stress state on the

yield surface. This corresponds to stress states lying on the saturated isotropic compression line for the MIT-E3 model, and the exact values of the mean effective stress p for any given increment of volumetric strain $\delta\varepsilon_v$ can be found using Equation (2), provided that the initial values of the mean effective stress p_0 and the specific volume v_0 are also known, together with the model parameters.

$$p = p_0 \exp\left(\frac{v_0(1 - \exp(-\delta\varepsilon_v))}{\lambda}\right) \quad (2)$$

To assess the accuracy of each integration method, the relative error in the stresses (i.e. err) is plotted against the volumetric strain size using double logarithmic scales, as shown in Figure 3. This facilitates a partial verification of the substepping strain-driven algorithm because, the gradient obtained for the straight line through a particular set of results, should correspond to the order of accuracy of the integration method (Lloret-Cabot *et al.* 2016). This follows from the fact that a numerical method has order of accuracy q (e.g. 1 for FE, 2 for ME, and 5 for RK) if the local truncation error err is $O(h^{q+1})$ for sufficiently small size h . This information can be used not only to verify the correctness of the algorithmic formulation but also to check and discuss its performance such as accuracy and efficiency (Gens and Potts 1988, Lloret-Cabot *et al.* 2016). Figure 3 shows the relative error converges at the expected rate (order of accuracy) of each numerical method, suggesting correct implementation. For example, approximate of gradients (i.e. 2, 3, 5, and 6) are obtained on the straight lines for the respective integration methods (i.e. FE, ME, RK4, and RK5).

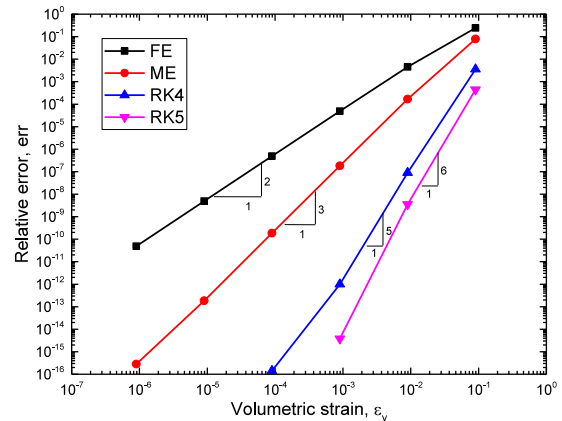


Figure 3. Relative error in stresses for single-step explicit integration scheme

The error behaviour is further investigated in the substepping schemes for the FE method with constant step size, and the ME and RK methods with error control, for a single volumetric strain increment of 9% (3% in each direction). Four constant substepping sizes ($d\varepsilon_{limit} = 10^{-6}, 10^{-5}, 10^{-4}, 10^{-3}$) are selected for the FE

method, and a wide range of error tolerance S_{TOL} (i.e., from 10^{-10} to 10^{-2}) are considered for the ME and RK methods in the analysis, which is sufficient for practical application. The values of relative errors plotted in Figure 4 corresponds to the accumulated contribution of local error (i.e. err , the error incurred by the numerical scheme in a single substep, e.g. Figure 3) at each substep and hence represents the total error behavior (i.e. Err , interpreted as the local error accumulated over a number of substeps). Consequently, at the end of substepping, the sum of all substep sizes integrated should be equal to the volumetric strain increment prescribed (i.e. 9%), and the corresponding relative error is the total error for this strain increment. The accumulated error is proportional to $\log n$ in the double-log plot, as demonstrated in Figure 4 with the substepping number.

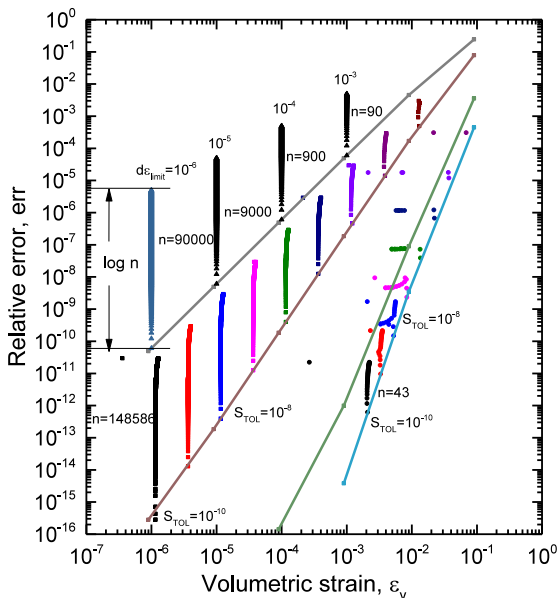


Figure 4. Relative error behaviour for three different substepping methods at different error tolerance

The CPU time for the element tests is too small (e.g. 0.1s) to compare the efficiency of these integration methods. Instead, the number of substeps from these methods for the same prescribed strain increment can be used as a proxy for the potential CPU time used in the analysis of boundary value problems. Figure 5 shows there are significant differences in the number of substeps n for ME and RK methods used for the 9% strain increment over a wide range of error tolerance, $S_{TOL} = 10^{-10} \sim 10^{-2}$. The number of substeps used in the FE method is indicated in Figure 4, which is simply the total strain divided by the substep size, $|\delta\epsilon|/d\epsilon_{limit}$. For a simple comparison, at the same total error, $Err = 10^{-5}$, achieved in the FE method with a small strain increment size $d\epsilon = 10^{-6}$, the number of substeps used in the FE, ME and RK methods is 90000, 235, and 9, respectively,

highlighting the inefficiency of FE method comparing to ME and RK methods.

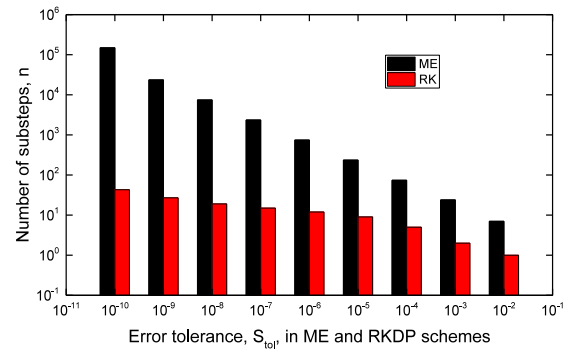


Figure 5. Variation of the number of substeps with the specified error tolerance

6 PERFORMANCE IN BOUNDARY VALUE PROBLEM

The undrained resistance of deeply-embedded pile/pipe section in homogeneous clay, is conducted to investigate the performance of the substepping scheme. It also has practical significance to derive the limiting pressure on laterally loaded vertical piles and vertically loaded horizontal pipes embedded in deep cohesive soils. The geometry and mesh of this analysis is shown in Figure 6, and plane strain condition is assumed considering that the pile/pipe is long. Quadratic elements (CPE6MPH) are used in the analysis for more accurate results in undrained condition. The ground is set as weightless in K_0 -normally consolidated state (with a consolidation stress $\sigma'_p = 100kPa$, $K_0 = 0.5344$, $OCR = 1$), and zero initial pore water pressure.

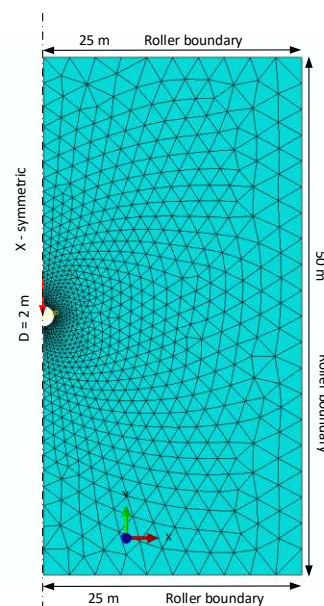


Figure 6. Finite element model of the deeply embedded rigid pile/pipe section in soils

Randolph and Houlsby (1984) derived analytical lower and upper bound solutions for the lateral resistance in isotropic soils by the method of characteristics. The limiting pressure factor N_p is reported in Equation (3),

$$N_p = \frac{P}{s_u D} = \pi + 2\Delta + \cos\left(\frac{\pi}{4} - \frac{\Delta}{4}\right) \left(\sqrt{2} + \sin\left(\frac{\pi}{4} - \frac{\Delta}{4}\right) \right) \quad (3)$$

where P is the applied lateral load, D is the diameter of the section, s_u is the undrained shear strength of the clay, $\sin \Delta = f_s/s_u$ is the interface roughness ratio, f_s is the limiting shear stress at the interface.

Ukritchon (1998) studied this problem in both isotropic and anisotropic soils using the finite element limit analysis and the anisotropic criterion by Davis and Christian (1971). The isotropic case is the same as the lateral loading of vertical pile section in Randolph and Houlsby (1984), whereas the anisotropic case is more related to the vertically loaded pipe section in deep soils and the T-bar penetration tests in geotechnical site investigation (Stewart and Randolph 1994). For anisotropic soils, the modified limiting pressure factor N'_p is defined in Equation (4),

$$\frac{P}{D} = N'_p \bar{s}_u = N'_p \frac{(s_{u,0^\circ} + s_{u,90^\circ})}{2} \quad (4)$$

where $s_{u,0^\circ}, s_{u,90^\circ}$ are the undrained strength at $\delta = 0^\circ, 90^\circ$ for the direction of the major principal stress δ relative to the vertical depositional axis (equivalent to $s_{u,v}$ and $s_{u,h}$), and \bar{s}_u is the average strength between compressive and extensive loading conditions.

The normalised load-displacement curves from the analyses using three integration methods (with the same error tolerances in the element tests) are presented in Figure 7, in both isotropic and anisotropic soils with smooth and rough interface. For the isotropic case, the resistance factor N_p is slightly below the analytical solution with both smooth and rough interface, based on the peak strength $s_u/\sigma'_{vp} = 0.2196$. However, the computed anisotropic resistance factor N'_p is much smaller than the analytical solution from Ukritchon (1998), based on the average peak strength ratio $\bar{s}_u/\sigma'_{vp} = 0.265$. This is mainly caused by the non-associated flow rule and strain-softening behaviour of the MIT-E3 model. Similar softening effect was also reported in the literature (Einav and Randolph 2005, Randolph and Andersen 2006).

This test demonstrates that the explicit substepping scheme for the MIT-E3 model is stable and robust in this challenging analysis.

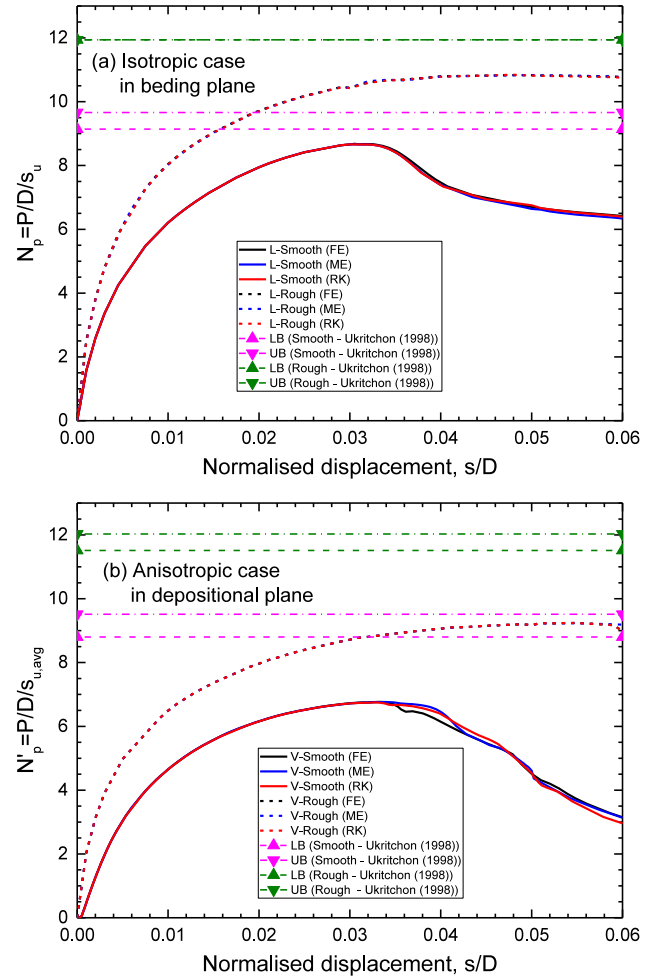


Figure 7. Normalised load-displacement response of deeply embedded rigid pile/pipe section

7 CONCLUSIONS

This paper presents the explicit substepping scheme to integrate the MIT-E3 model, and evaluate its performance systematically. General conclusions are drawn for future applications:

(a) The explicit substepping scheme is suitable for complex constitutive models such as the MIT-E3, where the implicit integration scheme is impractical. The accuracy of the integration can be controlled through adjusting the subincrement size for a strain increment.

(b) The FE method with very small subincrement size can be accurate in the finite element analysis, at the expense of large number of evaluation, which may not be efficient for large scale analysis. In addition, the substep size is not adaptive and cannot be determined accurately.

(c) The ME and RK methods with error control can adjust the subincrement size automatically through the specified local error tolerance, and thus versatile to balance the accuracy and efficiency requirements in practical applications.

(d) The deeply embedded pile/pipe section analysis shows that the explicit substepping scheme with error

control (i.e. ME and RK methods) is stable and robust in challenging analyses for the complex MIT-E3 model.

8 ACKNOWLEDGEMENTS

This research was initiated while working with Prof Andrew J. Whittle at the Singapore-MIT Alliance for Research and Technology (SMART), with financial support from the National Research Foundation (NRF) Singapore. The author is grateful to the late Prof. Scott W. Sloan to host his visit in Australia in 2016, and insightful discussions on the integration of complex constitutive models in the finite element framework.

9 REFERENCES

- Dafalias, Y.F., and Popov, E.P. 1975. A model of nonlinearly hardening materials for complex loading. *Acta Mechanica*, **21**(3): 173–192. Springer-Verlag. doi:10.1007/BF01181053.
- Davis, E.H., and Christian, J.T. 1971. Bearing Capacity of Anisotropic Cohesive Soil. *Journal of the Soil Mechanics and Foundations Division*, **97**(5): 753–769.
- Dormand, J.R., and Prince, P.J. 1980. A family of embedded Runge-Kutta formulae. *Journal of Computational and Applied Mathematics*, **6**(1): 19–26. doi:10.1016/0377-0427(86)90027-0.
- Dowell, M., and Jarratt, P. 1972. The “Pegasus” method for computing the root of an equation. *BIT*, **12**(4): 503–508. doi:10.1007/BF01932959.
- Einav, I., and Randolph, M.F. 2005. Combining upper bound and strain path methods for evaluating penetration resistance. *International Journal for Numerical Methods in Engineering*, **63**(14): 1991–2016. doi:10.1002/nme.1350.
- Gens, A., and Potts, D.M. 1988. Critical state models in computational geomechanics. *Engineering computations*, **5**(3): 178–197.
- Hashash, Y.M.A. 1992. Analysis of deep excavations in clay. Massachusetts Institute of Technology, Cambridge, Boston, U.S.
- Hueckel, T., and Nova, R. 1979. Some hysteresis effects of the behaviour of geologic media. *International Journal of Solids and Structures*, **15**(8): 625–642. doi:10.1016/0020-7683(79)90076-3.
- Kavvasdas, M.J. 1982. Non-linear consolidation around driven piles in clays. MIT, USA.
- Krieg, R.D. 1975. A Practical Two Surface Plasticity Theory. *Journal of Applied Mechanics*, **42**(3): 641. doi:10.1115/1.3423656.
- Ladd, C.C., and Foott, R. 1974. New Design Procedure for Stability of Soft Clays. *ASCE J Geotech Eng Div*, **100**(GT7): 763–786. doi:10.1061/ajgeb6.0000066.
- Lloret-Cabot, M., Sloan, S.W., Sheng, D., and Abbo, A.J. 2016. Error behaviour in explicit integration algorithms with automatic substepping. *International Journal for Numerical Methods in Engineering*, **108**(9): 1030–1053. doi:10.1002/nme.
- Lloret-Cabot, M., Wheeler, S.J., Gens, A., and Sloan, S.W. 2021. Numerical integration of an elasto-plastic critical state model for soils under unsaturated conditions. *Computers and Geotechnics*, **137**(December 2020): 104299. Elsevier Ltd. doi:10.1016/j.compgeo.2021.104299.
- Randolph, M.F., and Andersen, K.H. 2006. Numerical Simulation of T-Bar Penetration in Soft Clay. *International Journal of Geomechanics*, **6**(6): 411–420. doi:10.1061/40972(311)90.
- Randolph, M.F., and Houlsby, G.T. 1984. The limiting pressure on a circular pile loaded laterally in cohesive soil. *Géotechnique*, **34**(4): 613–623. Thomas Telford. doi:10.1680/geot.1984.34.4.613.
- Sloan, S.W. 1987. Substepping schemes for the numerical integration of elastoplastic stress-strain relations. *International Journal for Numerical Methods in Engineering*, **24**(5): 893–911. doi:10.1002/nme.1620240505.
- Sloan, S.W., Abbo, A.J., and Sheng, D. 2001. Refined explicit integration of elastoplastic models with automatic error control. *Engineering Computations*, **18**(1/2): 121–194. MCB UP Ltd. doi:10.1108/02644400110365842.
- Stewart, D.P., and Randolph, M.F. 1994. T-Bar Penetration Testing in Soft Clay. *Journal of Geotechnical Engineering - ASCE*, **120**(12): 2230–2235.
- Ukritchon, B. 1998. Application of numerical limit analyses for undrained stability problems in clay. MIT.
- Whittle, A.J. 1993. Evaluation of a constitutive model for overconsolidated clays. *Géotechnique*, **43**(2): 289–313.
- Whittle, A.J. 1995. Discussion: Evaluation of a constitutive model for overconsolidated clays. *Géotechnique*, **45**(1): 169–173. Thomas Telford. doi:10.1680/geot.1995.45.1.169.
- Whittle, A.J., Degroot, D.J., Ladd, C.C., and Tian-Ho, S. 1994. Model prediction of anisotropic behavior of Boston blue clay. *Journal of Geotechnical Engineering - ASCE*, **120**(2): 199–224.
- Whittle, A.J., and Kavvasdas, M.J. 1994. Formulation of MIT-E3 constitutive model for overconsolidated clays. *Journal of Geotechnical Engineering - ASCE*, **120**(1): 173–198.